JACS
JOURNAL OF THE AMERICAN CHEMICAL SOCIETY

Article

pubs.acs.org/JACS

Obtaining Two-Dimensional Electron Gas in Free Space without Resorting to Electron Doping: An Electride Based Design

Songtao Zhao, Zhenyu Li,* and Jinlong Yang*

Hefei National Laboratory for Physical Sciences at the Microscale and Synergetic Innovation Center of Quantum Information & Quantum Physics, University of Science and Technology of China, Hefei, Anhui 230026, China

Supporting Information

ABSTRACT: Nearly free electron (NFE) states are widely existed on atomically smooth surfaces in two-dimensional materials. Since they are mainly distributed in free space, these states can in principle provide ideal electron transport channels without nuclear scattering. Unfortunately, NFE states are typically unoccupied, and electron doping is required to shift them toward the Fermi level and, thus, to be involved in electron transport. Instead of occupying these NFE states, it is more desirable to have intrinsic nucleus-free two-dimensional electron gas in free space (2DEG-FS) at the Fermi level without relying on doping. Inspired by a recently identified electride material, we suggest that Ca_2N monolayer should possess such a 2DEG-FS state, which is then confirmed by our first-principles calculations. Phonon dispersion in Ca_2N monolayer shows no imagery frequency indicating that the monolayer structure is stable. A mechanical analysis demonstrates that Ca_2N bulk exfoliation is feasible to produce a freestanding monolayer. However, in real applications, the strong chemical activity of 2DEG-FS may become a practical issue. It is found that some ambient molecules can dissociatively adsorb on the Ca_2N monolayer, accompanying with a significant charge transfer from the 2DEG-FS state to adsorbates. To protect the 2DEG-FS state from molecule adsorption, we predict that graphane can be used as an effective encapsulating material. A well-encapsulated intrinsic 2DEG-FS state is expected to play an important role in low-dimensional electronics by realizing nuclear scattering free transport.

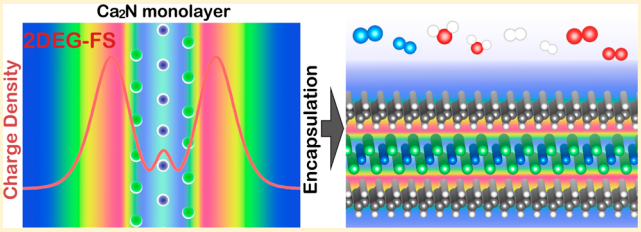

1. INTRODUCTION

During the minimization of electronic devices, an ultimate goal is shrinking their thickness to atomic scale.[1] When electronics really goes to the two-dimensional (2D) region, surface is expected to play an important role in the device design. An interesting example is making electron transport proceed mainly above the surface, thus nuclear scattering free. When scattering from nuclei is avoided, a significantly longer transport relaxation time can be obtained,[2] which is very helpful in minimizing electron resistance and heat generation.

Previous proposals for low dimensional nucleus-free electron transport channel rely on an interesting class of electronic states called nearly free electron (NFE) states.[2−4] NFE states were originally found in graphite and graphite intercalation compounds as a general interlayer bonding state with nearly free dispersion parallel to the graphitic planes.[5] It was then found that NFE states also exist in single layer graphene,[5,6] nanotubes,[2,3] and fullerenes,[7] possibly being Rydberg-like states bound by image potential.[8,9] Notice that NFE states mentioned here and the well-known NFE approximation[10] in electronic structure theory are not the same thing. NFE states have a unique real space distribution and thus special transport properties compared to conventional electronic states.

NFE states are typically several electronvolts above the Fermi level in energy. Therefore, electron transport is expected to mainly go through other states, such as covalently conjugated π bands in graphene, instead of the unoccupied NFE states. To be used as a transport channel, NFE states should be lowered in energy first. Electron doping is a possible way to stabilize NFE states.[3,11] When an NFE state becomes partially occupied, the resulting two-dimensional electron gas (2DEG) state is readily to be used as an effective transport channel.[12,13] At the same time, occupation of NFE states may also impart novel properties, such as superconductivity,[14] in low dimensional materials.

Although it can be used to occupy NFE states, doping either destroys the nuclear-scattering-free transport character (chemical doping) or involves complicated gate structures (electric doping). Therefore, intrinsic 2DEG-FS states in a neutral system without relying on doping is an interesting goal to pursue. This concept is closely related to an interesting system named electride where electrons served as anions.[15−17] Our first-principles calculations[18−20] have directly demonstrated that anionic electrons in electride are mainly distributed in free space. The recent success in synthesis of thermally stable electride materials[21,22] makes applications of electride ranging from field emission[23] to catalysis[24] possible.

The physical properties of anionic electrons are determined by the topology of the cavities confining them.[17] In early

Received: June 28, 2014
Published: September 4, 2014

   dx.doi.org/10.1021/ja5065125 | J. Am. Chem. Soc. 2014, 136, 13313−13318

studies, the space confining anionic electrons in electrides have been limited to zero-dimensional cavities and one-dimensionally linked channels. Recently, a layered electride material, dicalcium nitride, with 2D anionic electrons has been reported.[25] Its layered structure is expected to make further fabrication and processing easier compared to previous electride materials.

This new electride has a chemical formula of Ca_2N, or written as $[Ca_2N]^+e^-$ to reflect the anionic electron delocalized in the interstitial space between two Ca_2N layers. Ca_2N single crystal has an electrically resistive surface where conducting electrons are beneath the topmost $[Ca_2N]^+$ slab.[25] To expose 2DEG-FS in this electride material, we propose to use a Ca_2N monolayer. The possibility of obtaining monolayers via bulk exfoliation can be analyzed based on the cleavage energy and strength.

The Ca_2N electride is chemically very active.[26] To use the 2DEG-FS state of a Ca_2N monolayer in a realistic environment, a protection layer is required. As an ultimate membrane, graphene has been used as a chemical protect for metal corrosion.[27] However, it is not expected to be a good choice here due to a possible charge transfer from Ca_2N which will deplete the 2DEG-FS state. A more natural choice is an insulating 2D atomic layer, such as the boron nitride (BN) monolayer or graphane.

In this article, the possibility of Ca_2N exfoliation is discussed from a mechanical point of view. The electronic structure and transport properties of Ca_2N monolayer are systematically investigated via first-principles calculations. 2DEG-FS is observed on both surfaces of the Ca_2N monolayer, which makes the system very active. Graphane turns out to be a good protecting material for the 2DEG-FS. Effects of molecule adsorption can be effectively isolated by its thickness.

2. COMPUTATIONAL DETAILS

First-principles calculations were performed based on the density functional theory (DFT) implemented in the Vienna ab initio simulation package (VASP).[28,29] The projector-augmented wave (PAW) method[30,31] was used to describe the electron−ion interaction. The generalized gradient approximation in its Perdew, Burke, and Ernzerhof form (GGA-PBE)[32] was used for the exchange-correlation part of the electron−electron interaction. To describe the long-range van der Waals interaction, a correction to the total energy (DFT-D2)[33] was applied. The plane-wave energy cutoff was set to 500 eV.

To study 2D systems under the periodic boundary condition, a vacuum layer with a thickness at least 18 Å was inserted into the simulation cell. All the geometry structures were fully relaxed until energy and force were converged to 10^{-5} eV and 0.01 eV/Å, respectively. A series of unit cells were scanned for each system to obtain the in-plane lattice parameter. The obtained results (3.57, 2.47, 2.51, and 2.53 Å for monolayer Ca_2N, graphene, BN monolayer, and graphane) agree well with previous studies.[34−37]

A 15 × 15 and 29 × 29 Monkhorst−Pack *k*-point sampling[38] was used for Ca_2N monolayer geometry optimization and static electronic structure calculation, respectively. Molecule absorption on the Ca_2N monolayer surface was simulated using a 5 × 5 supercell, which matches well with the 7 × 7 supercell of graphene, BN monolayer, and graphane (Figure 1). The lattice parameter used for Ca_2N nanocomposite stacking with graphene, BN, and graphane (abbreviated as g/Ca_2N/g, BN/Ca_2N/BN, and G/Ca_2N/G) was 17.50, 17.70, and 17.75 Å, respectively. The corresponding lattice mismatch is less than 2% in all cases. In supercell calculations, the *k*-point mesh used for geometry optimization and static calculation was 3 × 3 and 5 × 5, respectively.

Bader's atom in molecule (AIM) method based on electron density topological analysis[39] was used to calculate charge populations.

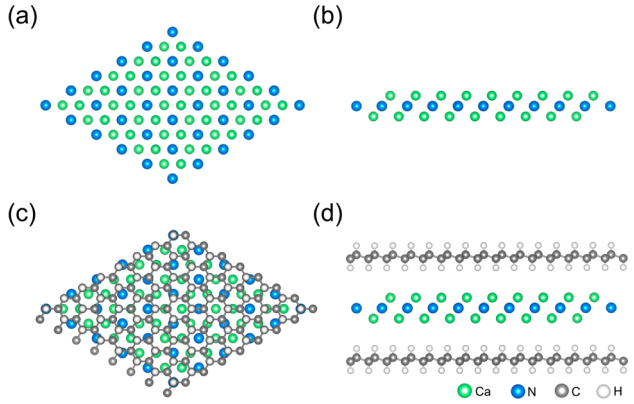

Figure 1. (a) Top and (b) side views of a 5 × 5 supercell of the Ca_2N monolayer. (c) Top and (d) side views of the G/Ca_2N/G supercell, corresponding to a 5 × 5 Ca_2N cell and a 7 × 7 graphane cell. The green, blue, gray, and white balls denote calcium, nitrogen, carbon, and hydrogen atoms, respectively.

Binding energy (E_b) was defined as energy of the combined system minus the energy sum for component systems. Therefore, more negative the binding energy more stable the combined system. Phonon dispersion analysis was performed using the Phonopy code[40] interfaced with the density functional perturbation theory[41] implemented in VASP. In phonon calculations, an increased plane-wave energy cutoff of 650 eV and a 39 × 39 *k*-point sampling were employed, accompanying with more stringent convergence criteria (10^{-8} eV for total energy and 10^{-8} eV/Å for Hellmann−Feynman Force). A first-principles molecular dynamics (MD) simulation in the canonical (NVT) ensemble was performed at 300 K with a Nosé thermostat.[42] The time step adopted in our MD simulation was 1.0 fs.

3. RESULTS AND DISSCUSSION

3.1. Stability and Exfoliation. Before calculating its electronic structure, we first check the stability of the Ca_2N monolayer. For this purpose, its phonon band structure is calculated. There are three atoms in a unit cell, which gives nine phonon dispersion bands (three acoustic modes and six optical modes). In Figure 2, longitudinal modes are plotted in red and doubly degenerated transverse modes are marked in blue. No imaginary frequency phonon is found at any wave vector, which

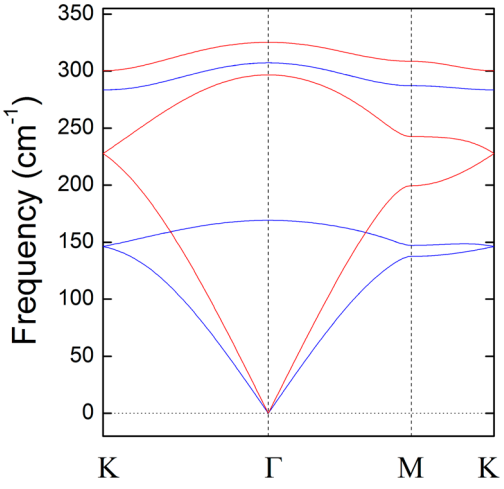

Figure 2. Phonon band structure of the Ca_2N monolayer. Longitudinal modes are marked in red while doubly degenerated transverse modes are in blue.

dx.doi.org/10.1021/ja5065125 | J. Am. Chem. Soc. 2014, 136, 13313−13318

confirms the dynamical stability of the 2D Ca_2N monolayer. At the same time, we also perform a first-principles MD simulation at 300 K for 2.5 ps using an 8 × 8 supercell, which suggests that the monolayer structure is quite stable at this temperature (Supporting Information Figure S1).

A practically very important issue related to the stability of a 2D atomic crystal is its capability of forming a freestanding membrane. To check if it is strong enough to avoid curling and allow the material to withstand its own weight or external load, we calculate the in-plane stiffness of the Ca_2N monolayer characterized by the 2D Young's modulus Y_{2D}. From the energy curve under axial strains (Supporting Information Figure S2),[43] the Y_{2D} of Ca_2N monolayer is calculated to be 0.35 eV/Å^2. If we estimate the deformation of Ca_2N sliver under gravity from the elastic theory by balancing gravity and 2D strain energy,[44] we obtained a ratio between the vertical deformation and dimension of the freestanding Ca_2N sheet as small as 10^{-3} to 10^{-4} even for large flakes about 10^4 μm^2 (see Supporting Information for more details). This result demonstrates that Ca_2N monolayer is strong enough to produce a freestanding 2D membrane without the support of a substrate.

Confirmed that Ca_2N monolayer is a stable structure with a high mechanical strength, we then check the possibility of obtaining Ca_2N monolayers via a mechanical exfoliation. The Ca_2N bulk is built up from ABC stacking atomic layers. Each layer is composed of an N atom plane sandwiched by two Ca-atom planes (Figure 1b). Thermodynamically, the exfoliation process should overcome a cleavage energy E_{cl} determined by the interlayer coupling strength.[45] To calculate the cleavage energy, a fracture is introduced in the unit cell of Ca_2N bulk. Notice that the Ca_2N unit cell is already large enough to avoid the artificial interaction between two neighboring fractures. The calculated cleavage energy E_{cl} is 1.09 J/m^2.

If we perform a scan on the separation distance d of the fracture, the theoretical cleavage strength σ can be obtained as the maximum derivative of E_{cl} (Figure 3).[45] The calculated cleavage strength is 4.42 GPa. We have also simulated the separation of a Ca_2N monolayer from a neighboring trilayer (inset of Figure 3). The corresponding cleavage energy and strength are very similar to the bulk cleavage case, indicating

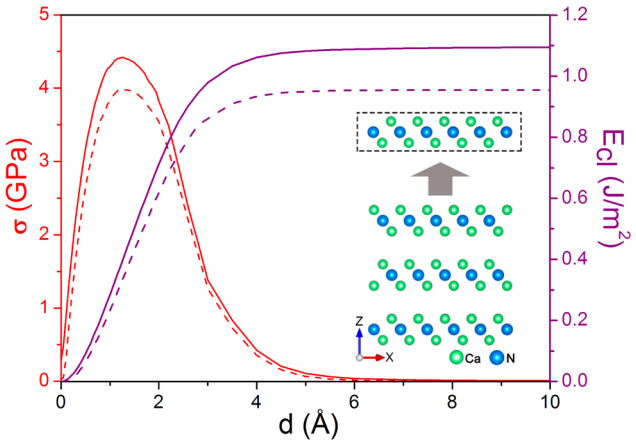

Figure 3. Cleavage energy E_{cl} in J/m^2 (purple lines) and its derivative σ in GPa (red lines) as a function of the separation distance d for a fracture in Ca_2N bulk. Solid and dash lines correspond to results obtained with and without the van der Waals D2 correction, respectively. Inset: Separating a monolayer from its neighboring trilayer.

that the exfoliation process is not very sensitive to the number of layers.

By comparing the calculated cleavage energy and strength with corresponding values in typical layered materials, we can judge if exfoliation of Ca_2N is feasible. The cleavage energy of Ca_2N is comparable to the experimentally estimated E_{cl} value of graphite (0.37 J/m^2).[46] According to our calculations, the cleavage strength of graphite is 2.10 GPa, also not very different from Ca_2N. Since graphene[47] and many other materials[48] can be exfoliated to obtain 2D atomic crystals, we expected that Ca_2N, with a similar cleavage energy and strength, will also be able to be exfoliated by either Scotch tape or atomic force microscopy tip.[49] Notice that, although the exfoliation process discussed here can be routinely used in laboratory, an effective way to produce Ca_2N monolayer samples in industry is still an interesting goal to pursue.

3.2. 2DEG-FS State. There are two Ca atoms and one N atom in the unit cell of Ca_2N monolayer with 21 valence electrons. Its ground-state band structure is shown in Figure 4a,

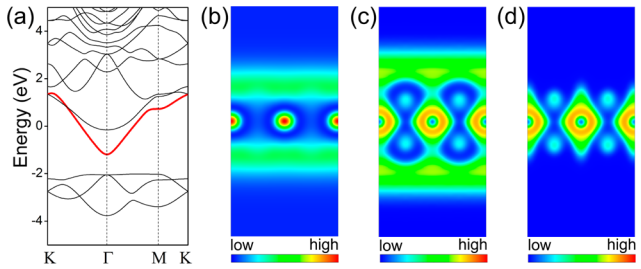

Figure 4. Calculated electronic structure of Ca_2N monolayer. (a) Band structure with the Fermi energy set to zero. The 2DEG-FS band is marked in red. (b) Band decomposed electron density map of the 2DEG-FS band at the Γ point. The maximum electronic density is 0.0164 e/Å^3. ELF maps of (c) Ca_2N and (d) $[Ca_2N]^+$ with a scale bar from zero at the low end to one at the high end.

where no spin polarization is found. There is a partially occupied band crossing the Fermi level with a large in-plane dispersion, similar to the bulk case.[25] Its density map at the Γ point (Figure 4b) clearly shows that electron is delocalized above both surfaces of the Ca_2N plane. Therefore, it is a 2DEG-FS state.

The degree of electron localization can be quantitatively described by an electron-localization function (ELF)[50] which equals to 1 for strong localization and 1/2 for a uniform electron gas. On both sides of the Ca_2N plane, a delocalized ELF feature is clearly shown in Figure 4c. Notice that ELF can also be used to characterize the bonding type.[16,51] For Ca_2N monolayer, there is no bonding localization attractor on the bond path between $[Ca_2N]^+$ and e^-. Therefore, the delocalized 2D electron forms ionic bond with the atomic plane and the Ca_2N monolayer is an electride too.

For $[Ca_2N]^+$ with one valence electron removed, the delocalized ELF features on the surfaces are totally disappeared. Therefore, electron transfer from Ca_2N monolayer will first vacate the 2DEG-FS state. This result confirms that the 2DEG-FS state can be really used as an effective transport channel. The band structure calculation for $[Ca_2N]^+$ gives a consistent result, predicting an energy gap formation with unoccupied NFE conductance bands (Supporting Information Figure S8).

Compared to typical 2D electronic systems, such as GaAs–AlGaAs heterojunction, $LaAlO_3$–$SrTiO_3$ interface,[52] and graphene,[53] the 2DEG-FS state in Ca_2N monolayer provides

dx.doi.org/10.1021/ja5065125 | J. Am. Chem. Soc. 2014, 136, 13313–13318

a fairly high carrier concentration (8.9×10^{14} electron/cm^2). The effective mass m^* at the Fermi level is about $1.44m_e$, where m_e is the mass of free electrons. Since Ca_2N bulk is a layered materials and exfoliation should not introduce strong boundary scattering, we use the experimental transport relaxation time of Ca_2N bulk[25] to estimate the mobility μ of the Ca_2N monolayer. The obtained value is about 730 cm^2 V^{-1} s^{-1}. This is comparable to μ in oxide interface (Supporting Information Table S1), and about 1 order of magnitude larger than Ag at room temperature (67 cm^2 V^{-1} s^{-1}).[54]

Notice that in a low-dimensional system with a high electron density, the electron−electron scattering becomes not negligible, which makes it difficult to obtain a very high mobility. With a nuclear-scattering-free character, we believe that the mobility of the Ca_2N monolayer is among the highest in 2D materials with a similar carrier density. Intrinsic 2DEG-FS states thus open a new avenue to improve the mobility and carrier density in a balanced way in low-dimensional materials.

Although the 2DEG-FS state in Ca_2N monolayer provides an ideal transport channel without nuclear scattering, it is expected to be too chemically active to survive in the ambient environment. Adsorption of small molecules on Ca_2N monolayer surface is studied within a 5×5 supercell. For all the four molecules considered here, the calculated binding energies (Table 1) are negatively large, which indicates a large thermodynamic driving force for adsorption.

Table 1. Binding Energy (E_b) and Charge Transfer (q_t) for Different Molecule Adsorptions[a]

	H_2	H_2O	N_2	O_2
E_b(eV)	−1.571	−2.168	−0.810	−8.535
q_t(e)	1.523	0.658	1.466	2.858
E_b' (eV)	−0.004	−0.015	−0.004	−0.467
q_t' (e)	0.001	0.001	0.001	0.410

[a]A negative sign in q_t corresponds to electron transfer from the adsorbate to the substrate. E_b' and q_t' are binding energy and charge transfer for molecular adsorption on G/Ca_2N/G.

Upon adsorption, the N_2 molecule is stretched from 1.12 to 1.25 Å. A significant charge transfer (about 1.5 electron per N_2 molecule) from Ca_2N to N_2 is also observed. For molecules more active than N_2, a dissociative adsorption is observed. Both H_2 and O_2 molecules are cleaved into two atoms, which bind strongly with the Ca_2N monolayer surface. H_2O is cleaved into H and OH upon adsorption. H enters the Ca_2N lattice and binds to an N atom, while OH is adsorbed at a hollow site (Supporting Information Figure S9). These results are consistent with spontaneous oxidation and explosive reaction with H_2O to produce ammonia and an oxide from Ca_2N in experiment.[26]

3.3. Encapsulation. Since 2DEG-FS is chemically very active, an effective encapsulation is required for electronics applications of the Ca_2N monolayer in an ambient environment. To select a suitable encapsulating material, two conditions should be fulfilled. First, it should not react with the 2DEG-FS state itself. Second, adsorption of ambient molecules on it should not affect the underlying 2DEG-FS either. With these two conditions fulfilled, thinner 2D materials are preferred.

Graphene is the most famous 2D atomic layer. In graphene covered Ca_2N monolayer system (g/Ca_2N/g), a significant electron transfer from Ca_2N to graphene is observed (Table 2).

Table 2. Binding Energy (E_b), Interlayer Distance (D), and Charge Transfer (q_t) between the Ca_2N Monolayer and Its Encapsulating Material[a]

	g/Ca2N/g	BN/Ca_2N/BN	G/Ca_2N/G
E_b (eV)	−42.63	−10.71	−3.57
D (Å)	2.54	2.66	3.54
q_t (e)	18.81	17.39	2.86

[a]A negative sign in q_t corresponds to electron transfer from the encapsulating material to Ca_2N.

The 2DEG-FS state of Ca_2N monolayer becomes unoccupied and strongly hybridized with graphene states. Therefore, graphene cannot be used as an encapsulating material for the Ca_2N monolayer.

A possible way to suppress the charge transfer is resorting to materials with a large band gap, e.g., BN monolayer. Our first-principles calculations have really found that BN can form a weakly binding 2D composite material with the Ca_2N monolayer. However, such a weakly bound state is only a local minimum of the potential energy surface (Supporting Information Figure S13). In the ground state geometry of BN/Ca_2N/BN with a smaller interlayer distance (Supporting Information Figure S16), the BN layers are slightly distorted, indicating a strong interaction. Even starting from the weakly bound state, upon O_2 adsorption, the interlayer distance can spontaneously decrease toward the ground-state value.

To provide an effective protection to the 2DEG-FS state, we then consider a thicker 2D atomic sheet, graphane, also with a wide band gap. The graphane covered Ca_2N monolayer, G/Ca_2N/G, has a binding energy of −3.57 eV per supercell (about 0.07 eV per Ca atom) with an equilibrium interlayer spacing of about 3.54 Å. Therefore, interaction between graphane and the Ca_2N monolayer is very weak, a typical van der Waals interaction. An energy scan of the interlayer distance finds no other stable state with a stronger chemical interaction between graphane and the Ca_2N monolayer (Supporting Information Figure S13).

The band structure of G/Ca_2N/G (Figure 5a) is fully consistent with such a weak interaction picture. It is almost a rigid combination of the band structures of graphane and the Ca_2N monolayer. Due to the supercell-induced band folding, the original 2DEG-FS band becomes several bands here, and the lowest one is marked in red in Figure 5. Below that, there are several bands originated from graphane. The Fermi level position remains the same compared to the band structure of the Ca_2N monolayer (Supporting Information Figure S17), which indicates that there is very little charge transfer in the system. Bader population analysis gives a charge transfer from Ca_2N to graphane only 0.057 electron per Ca atom. ELF map (Figure 5b) also clearly shows the existence of delocalized interlayer electrons. Therefore, graphane encapsulation does not affect the partially occupied 2DEG-FS state of Ca_2N monolayer, and the transport properties of the Ca_2N monolayer will be well kept in G/Ca_2N/G.

Adsorption of ambient molecules on G/Ca_2N/G is also studied. As listed in Table 1, the binding energies of N_2, H_2O, and H_2 are very small, suggesting a weak physical adsorption. For O_2, the binding energy is about −0.47 eV, and there is a 0.41 electron charge transfer from G/Ca_2N/G to O_2. Therefore, it deserves a further analysis to see if the 2DEG-FS state is affected by the O_2 adsorption. From the band structure (Figure 5c), we do not see any notable influence on

dx.doi.org/10.1021/ja5065125 | J. Am. Chem. Soc. 2014, 136, 13313−13318

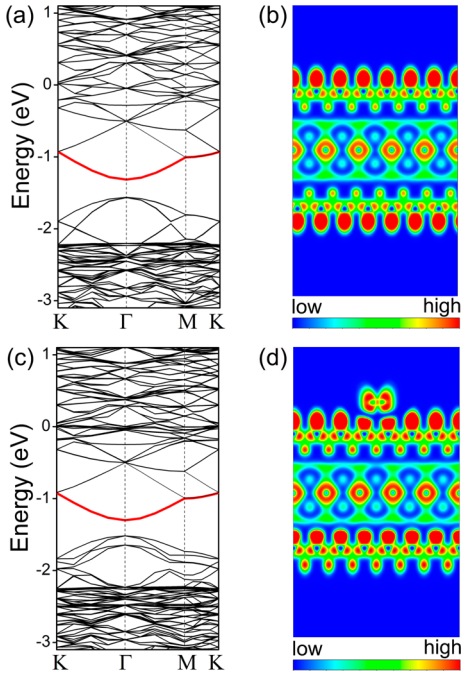

Figure 5. (a) Band structure and (b) ELF map of G/Ca_2N/G. (c) Band structure and (d) ELF map of oxygen adsorbed G/Ca_2N/G. The ELF scale bar is from 0.1 to 0.9. The lowest 2DEG-FS band is marked in red. The Fermi level is set to zero.

the 2DEG-FS band upon the oxygen adsorption. Only those bands originated from graphane are notably changed. ELF map (Figure 5d) also supports such a picture where O_2 only interacts with graphane and O_2 adsorption has little effect on the encapsulated Ca_2N monolayer. Charge transfer between Ca_2N and O_2 adsorbed graphane is almost the same as that between Ca_2N and a pristine graphane. Therefore, G/Ca_2N/G provides a well encapsulation for 2DEG-FS even when ambient molecules are adsorbed on it.

4. CONCLUSION

In summary, we have designed a new 2D material, Ca_2N monolayer, with a partially occupied 2DEG-FS state. The calculated phonon dispersion proves its stability and the mechanical analysis suggests that exfoliation of the Ca_2N bulk to obtain freestanding monolayers is feasible. The 2DEG-FS state on the Ca_2N monolayer surface provides a nuclear-scattering-free transport channel, which provides a unique way to improve the mobility in low dimensional materials with a high carrier density. However, to use it in an ambient environment, an effective encapsulation is required. Graphane has been found interacting weakly with the Ca_2N monolayer, and the 2DEG-FS state remains intact upon ambient molecule adsorption if a graphane protection is provided. Since the 2DEG-FS state can transport electron at nano scale via a new paradigm totally different from the traditional through-bond picture, the results obtained in this study will have an important impact on future nanoscience and engineering.

■ ASSOCIATED CONTENT

Ⓢ Supporting Information

More figures and data for geometry, mechanical analysis, and electronic structure calculations. This material is available free of charge via the Internet at http://pubs.acs.org.

■ AUTHOR INFORMATION

Corresponding Authors

zyli@ustc.edu.cn
jlyang@ustc.edu.cn

Notes

The authors declare no competing financial interest.

■ ACKNOWLEDGMENTS

This work is partially supported by MOST (2011CB921404 and 2014CB932700), by NSFC(21222304, 21173202, and 21121003), by CAS (XDB01020300), by CUSF, and by USTC-SCC, SCCAS, Tianjin, and Shanghai Supercomputer Centers.

■ REFERENCES

(1) Schwierz, F. *Nat. Nanotechnol.* **2010**, *5*, 487.
(2) Okada, S.; Oshiyama, A.; Saito, S. *Phys. Rev. B* **2000**, *62*, 7634.
(3) Hu, S.; Zhao, J.; Jin, Y.; Yang, J.; Petek, H.; Hou, J. *Nano Lett.* **2010**, *10*, 4830.
(4) Lu, N.; Li, Z.; Yang, J. *J. Phys. Chem. C* **2009**, *113*, 16741.
(5) Posternak, M.; Baldereschi, A.; Freeman, A.; Wimmer, E.; Weinert, M. *Phys. Rev. Lett.* **1983**, *50*, 761.
(6) Silkin, V.; Zhao, J.; Guinea, F.; Chulkov, E.; Echenique, P.; Petek, H. *Phys. Rev. B* **2009**, *80*, 121408.
(7) Feng, M.; Zhao, J.; Petek, H. *Science* **2008**, *320*, 359.
(8) Feng, M.; Zhao, J.; Huang, T.; Zhu, X.; Petek, H. *Acc. Chem. Res.* **2011**, *44*, 360.
(9) Echenique, P.; Pendry, J. *J. Phys. C: Solid State Phys.* **1978**, *11*, 2065.
(10) Kittel, C. *Introduction to Solid State Physics*, 8th ed.; John Wiley and Sons: New York, 2005, Chapter 7.
(11) Zhao, J.; Feng, M.; Yang, J.; Petek, H. *ACS Nano* **2009**, *3*, 853.
(12) Zhao, J.; Zheng, Q.; Petek, H.; Yang, J. *J. Phys. Chem. A* **2014**, *118*, 7255.
(13) Liu, Q.; Li, Z.; Yang, J. *Chin. J. Chem. Phys.* **2011**, *24*, 22.
(14) Csányi, G.; Littlewood, P.; Nevidomskyy, A. H.; Pickard, C. J.; Simons, B. *Nat. Phys.* **2005**, *1*, 42.
(15) Huang, R. H.; Faber, M. K.; Moeggenborg, K. J.; Ward, D. L.; Dye, J. L. *Nature* **1988**, *331*, 599.
(16) Dye, J. L. *Science* **2003**, *301*, 607.
(17) Dye, J. L. *Acc. Chem. Res.* **2009**, *42*, 1564.
(18) Li, Z.; Yang, J.; Hou, J.; Zhu, Q. *J. Am. Chem. Soc.* **2003**, *125*, 6050.
(19) Li, Z.; Yang, J.; Hou, J.; Zhu, Q. *Angew. Chem., Int. Ed.* **2004**, *43*, 6479.
(20) Li, Z.; Yang, J.; Hou, J.; Zhu, Q. *Chem.—Eur. J.* **2004**, *10*, 1592.
(21) Matsuishi, S.; Toda, Y.; Miyakawa, M.; Hayashi, K.; Kamiya, T.; Hirano, M.; Tanaka, I.; Hosono, H. *Science* **2003**, *301*, 626.
(22) Redko, M. Y.; Jackson, J. E.; Huang, R. H.; Dye, J. L. *J. Am. Chem. Soc.* **2005**, *127*, 12416.
(23) Toda, Y.; Matsuishi, S.; Hayashi, K.; Ueda, K.; Kamiya, T.; Hirano, M.; Hosono, H. *Adv. Mater.* **2004**, *16*, 685.
(24) Kitano, M.; Inoue, Y.; Yamazaki, Y.; Hayashi, F.; Kanbara, S.; Matsuishi, S.; Yokoyama, T.; Kim, S.-W.; Hara, M.; Hosono, H. *Nat. Chem.* **2012**, *4*, 934.
(25) Lee, K.; Kim, S. W.; Toda, Y.; Matsuishi, S.; Hosono, H. *Nature* **2013**, *494*, 336.
(26) Gregory, D. H.; Bowman, A.; Baker, C. F.; Weston, D. P. *J. Mater. Chem.* **2000**, *10*, 1635.
(27) Prasai, D.; Tuberquia, J. C.; Harl, R. R.; Jennings, G. K.; Bolotin, K. I. *ACS Nano* **2012**, *6*, 1102.
(28) Kresse, G.; Furthmüller, J. *Comput. Mater. Sci.* **1996**, *6*, 15.
(29) Kresse, G.; Furthmüller, J. *Phys. Rev. B* **1996**, *54*, 11169.
(30) Blöchl, P. E. *Phys. Rev. B* **1994**, *50*, 17953.
(31) Kresse, G.; Joubert, D. *Phys. Rev. B* **1999**, *59*, 1758.
(32) Perdew, J. P.; Burke, K.; Ernzerhof, M. *Phys. Rev. Lett.* **1996**, *77*, 3865.

(33) Grimme, S. *J. Comput. Chem.* **2006**, *27*, 1787.
(34) Reckeweg, O.; DiSalvo, F. J. *Solid State Sci.* **2002**, *4*, 575.
(35) Neto, A. C.; Guinea, F.; Peres, N.; Novoselov, K. S.; Geim, A. K. *Rev. Mod. Phys.* **2009**, *81*, 109.
(36) Jiang, X.; Zhao, J.; Ahuja, R. *J. Phys.: Condens. Matter* **2013**, *25*, 122204.
(37) Sofo, J. O.; Chaudhari, A. S.; Barber, G. D. *Phys. Rev. B* **2007**, *75*, 153401.
(38) Methfessel, M.; Paxton, A. *Phys. Rev. B* **1989**, *40*, 3616.
(39) Sanville, E.; Kenny, S. D.; Smith, R.; Henkelman, G. *J. Comput. Chem.* **2007**, *28*, 899.
(40) Togo, A.; Oba, F.; Tanaka, I. *Phys. Rev. B* **2008**, *78*, 134106.
(41) Gonze, X.; Lee, C. *Phys. Rev. B* **1997**, *55*, 10355.
(42) Nosé, S. *J. Chem. Phys.* **1984**, *81*, 511.
(43) Sachs, B.; Wehling, T.; Novoselov, K.; Lichtenstein, A.; Katsnelson, M. *Phys. Rev. B* **2013**, *88*, 201402.
(44) Booth, T. J.; Blake, P.; Nair, R. R.; Jiang, D.; Hill, E. W.; Bangert, U.; Bleloch, A.; Gass, M.; Novoselov, K. S.; Katsnelson, M. I. *Nano Lett.* **2008**, *8*, 2442.
(45) Medvedeva, N.; Mryasov, O.; Gornostyrev, Y. N.; Novikov, D.; Freeman, A. *Phys. Rev. B* **1996**, *54*, 13506.
(46) Zacharia, R.; Ulbricht, H.; Hertel, T. *Phys. Rev. B* **2004**, *69*, 155406.
(47) Novoselov, K. S.; Geim, A. K.; Morozov, S.; Jiang, D.; Zhang, Y.; Dubonos, S.; Grigorieva, I.; Firsov, A. *Science* **2004**, *306*, 666.
(48) Novoselov, K.; Jiang, D.; Schedin, F.; Booth, T.; Khotkevich, V.; Morozov, S.; Geim, A. *Proc. Natl. Acad. Sci. U.S.A.* **2005**, *102*, 10451.
(49) Hong, S. S.; Kundhikanjana, W.; Cha, J. J.; Lai, K.; Kong, D.; Meister, S.; Kelly, M. A.; Shen, Z.-X.; Cui, Y. *Nano Lett.* **2010**, *10*, 3118.
(50) Becke, A. D.; Edgecombe, K. E. *J. Chem. Phys.* **1990**, *92*, 5397.
(51) Silvi, B.; Savin, A. *Nature* **1994**, *371*, 683.
(52) Mannhart, J.; Schlom, D. *Science* **2010**, *327*, 1607.
(53) Novoselov, K. S.; Geim, A. K.; Morozov, S. V.; Jiang, D.; Katsnelson, M. I.; Grigorieva, I. V.; Dubonos, S. V.; Firsov, A. A. *Nature* **2005**, *438*, 197.
(54) Kasap, S. O. *Principles of Electronic Materials and Devices, 3rd Ed.*; McGraw-Hill: New York, NY, 2006.